Calcium Ions as "Miscibility Switch": Colocalization of Surfactant Protein B with Anionic Lipids under Absolute Calcium Free Conditions

Mohammed Saleem,[†] Michaela C. Meyer,[†] Daniel Breitenstein,[‡] and Hans-Joachim Galla[†*]
[†]Institute of Biochemistry, University of Münster, Münster, Germany; and [‡]Tascon, Münster, Germany

ABSTRACT One of the main determinants of lung surfactant function is the complex interplay between its protein and lipid components. The lipid specificity of surfactant protein B (SP-B), however, and the protein's ability to selectively squeeze out lipids, has remained contradictory. In this work we present, for the first time to our knowledge, by means of time-of-flight secondary ion mass spectrometry chemical imaging, a direct evidence for colocalization of SP-B as well as its model peptide KL_4 with negatively charged dipalmitoylphosphatidylglycerol under absolute calcium free conditions. Our results prove that protein/lipid localization depends on the miscibility of all surfactant components, which itself is influenced by subphase ionic conditions. In contrast to our earlier studies reporting SP-B/KL_4 colocalization with zwitterionic dipalmitoylphosphatidylcholine, in the presence of even the smallest traces of calcium, we finally evidence an apparent reversal of protein/lipid mixing behavior upon calcium removal with ethylene diamine tetraacetic acid. In addition, scanning force microscopy measurements reveal that by depleting the subphase from calcium ions the protrusion formation ability of SP-B or KL_4 is not hampered. However, in the case of KL_4, distinct differences in protrusion morphology and height are visible. Our results support the idea that calcium ions act as a "miscibility switch" in surfactant model systems and probably are one of the major factors steering lipid/protein mixing behavior as well as influencing the protein's protrusion formation ability.

INTRODUCTION

The mammalian pulmonary surfactant, a complex lipid/protein mixture lining the alveolar/air interface of the lung, is crucial for lowering the surface tension and thus preventing alveolar collapse (1–3). It is primarily composed of phospholipids, especially dipalmitoylphosphatidylcholine (DPPC), phosphatidylglycerols (PG), unsaturated lipids, and small amounts of surfactant proteins (namely, SP-A, SP-B, SP-C, and SP-D (4,5)). Deficiency of pulmonary surfactant leads to respiratory distress syndrome, a leading cause for morbidity and mortality in premature infants (1,6). A significant amount of research has been undertaken to understand the mechanism of lung surfactant function, largely focusing upon the role of lipids, surfactant proteins and their model peptides (4,7–10), phase behavior (11–14), surface activity (3,15–17), and the structure-function relationship (16,18,19). In the case of SP-C it has been shown that for binary mixtures, SP-C is fully miscible with DPPC, whereas it leads to formation of domains with DPPG, suggesting a strong electrostatic interaction (20). In the more complex ternary mixtures containing both DPPC and DPPG, SP-C is found to coexist in networklike domain structures along with DPPC, which surrounds DPPG-rich domains (20). Studies on SP-B have shown that this protein remarkably increases surface adsorption of phospholipids; the nature of its interaction with these lipids, however, is still discussed controversially (21–23). Recent investigations have also dealt with a synthetic model peptide, i.e., [lysine-$(leucine)_4]_4$-lysine] (KL_4), designed to mimic the actions of SP-B. KL_4-containing lung surfactant formulations are currently tested in clinical trials as therapeutic agent for respiratory distress syndrome in premature infants (24). However, its mode of action and the role of specific peptide/lipid interactions for its effectiveness in medical treatment remain unclear.

Particularly interesting are the results found in literature concerning lipid specificities of surfactant proteins. The first instance for the existence of specific SP-B/DPPG interactions was proposed based on fluorescence anisotropy studies in lipid bilayers (13), followed by a model stating an interaction of SP-B with PG headgroups (16) and further electron paramagnetic resonance spectroscopy studies in vesicular systems (25). However, other bilayer studies using ^2H nuclear magnetic resonance suggested that SP-B showed no specific interaction with either DPPC or DPPG (26). Additionally, our most recent monolayer studies concerning SP-B and KL_4 interaction with specific lipids using time-of-flight secondary ion mass spectrometry (ToF-SIMS) demonstrated SP-B/DPPC (27,28) and likewise KL_4/DPPC colocalization (without, however, excluding the existence of specific DPPG/protein interactions) (29). The discrepancies in the existing results might be due to different experimental conditions and techniques used for studying lipid/protein interactions.

Our own studies performed in the last years all apply a well-established and standardized surfactant model system composed of DPPC/DPPG/protein monolayers. Furthermore, we systematically used powerful surface analysis tools such as ToF-SIMS and scanning force microscopy (SFM) and thus gained a broad insight on surfactant phase behavior under various subphase conditions (20,27–29). All our results showed a strong tendency of DPPG to form

Submitted December 11, 2008, and accepted for publication May 8, 2009.

*Correspondence: gallah@uni-muenster.de

Editor: Peter Hinterdorfer.

0006-3495/09/07/0500/9 $2.00

doi: 10.1016/j.bpj.2009.05.011

condensed circular domains from which DPPC and protein were excluded. Our suggestion was that traces of calcium present either in pure water (20,27) or buffered subphases (28) and the presence of high calcium contents (29) lead to bridging of the negatively charged headgroups, and thus, a demixing of the monolayer components. A missing link in our own experimental series, however, has been the verification of the lipid/protein mixing behavior under absolute calcium free conditions, e.g., guaranteed by the addition of ethylene diamine tetraacetic acid (EDTA) as a potent calcium chelator. This article summarizes the results of our ToF-SIMS and SFM studies with SP-B and KL_4-containing surfactant systems under calcium free conditions, which support our idea of calcium ions acting as a ''miscibility switch''. For the first time to our knowledge, direct evidence for colocalization of SP-B or KL_4 with a negatively charged lipid is provided for monolayer systems. Additionally, we report the influence of changes in the ionic environment on functional aspects such as the membrane-protrusion-forming ability of surfactant protein B and its model peptide KL_4.

MATERIAL AND METHODS

Lipids and proteins

The lipids used in this study, namely 1,2-dipalmitoyl-*sn*-glycero-3-phosphocholine (DPPC), 1,2-dipalmitoyl-*sn*-glycero-3-phosphoglycerol (DPPG), and 1,2-dipalmitoyl-D62-*sn*-glycero-3-phosphoglycerol (d62DPPG), were purchased from Avanti Polar Lipids (Alabaster, AL). A quantity of 2-(4,4-difluoro-5-methyl-4-bora-3a,4a-diaza-*s*-indacene-3-dodecanoyl)-1-hexadecanoyl-*sn*-glycero-3-phosphocholine (β-BODIPY 500/510 C_{12}-HPC) was obtained from Molecular Probes (Eugene, OR). All lipids were used without further purification. Chloroform, methanol, and hexane were HPLC grade and purchased from Roth (Karlsruhe, Germany). Water was purified and deionized by a multicartridge system (Millipore, Billerica, MA) and had a resistivity >18 M$\Omega\cdot$cm. A quantity of *n*-(2-hydroxyethyl) piperazine-*n*′-2-ethansulfonic acid (HEPES) was obtained from Sigma-Aldrich (Taufkirchen, Germany) and $CaCl_2$ from Merck (Darmstadt, Germany).

The porcine surfactant protein SP-B was purified from bronchoalveolar lavage fluid by butanol extraction (30). The protein was free of contaminants, as was evidenced by electrospray ionization mass spectrometry. The amino-acid sequence corresponds to the expected sequence according to the Swiss-Prot database (http://www.uniprot.org/). The SP-B model peptide KL_4 with the sequence KLLLLKLLLLKLLLLKLLLLK was obtained from Richard Mendelsohn (Rutgers University, Newark, NJ). The concentration of the peptide was estimated by fluorescamine assays. Lipids and peptides were dissolved in chloroform/methanol solution (1:1, v/v).

Preparation of gold supports

Preparation of gold supports was performed as described previously (20). Briefly, cleaned glass slides were treated with argon plasma in a plasma cleaner (PDC 32G-2; Harrick, Ossining, NY) for 3 min. Then 1 nm of chromium was deposited on the surface of the slide, serving as an adhesive layer, onto which 200 nm of gold were sublimed at a rate of 0.01 nm/s. The gold-covered slides were cleaned by rectification for 8 h in a Soxhlet apparatus using *n*-hexane.

Langmuir-Blodgett transfer

For ToF-SIMS and SFM investigations, surfactant monolayers were transferred to gold-coated glass slides and mica sheets (Electron Microscopy Science, Munich, Germany), respectively, using the Langmuir-Blodgett (LB) technique. The gold-coated substrates were cleaned with argon plasma in plasma cleaner before its use, to make sure that the substrate remains hydrophilic during the transfer procedure and successfully enable monolayer transfer. The respective substrate was dipped into the buffered subphase (25 mM HEPES, pH 7.0) containing 0.1 mM EDTA of a Wilhelmy-film balance (Riegler and Kirstein, Mainz, Germany) with an operational area of 39 cm^2 at a temperature of 20°C. Then the lipid/peptide mixture was spread from chloroform/methanol (1:1, v/v) solutions onto the surface. After an equilibration period of 10 min, the film was compressed with a velocity of 1.5 cm^2/min until a surface pressure of 50 mN/m was reached. The monolayer was then equilibrated for another 25 min at this surface pressure before transferring the film with a velocity of 0.7 mm/min.

Time-of-flight secondary ion mass spectrometry

Time-of-flight (ToF-SIMS) measurements of surface films transferred onto gold supports were obtained on a ToF-SIMS IV (IONTOF, Münster, Germany) using Bi_3^+ as primary ion at 25 keV. To unambiguously identify the detected surface components, spectra were taken in bunched mode (focus: 3–5 μm) with a mass resolution of 5000–10,000. Cycling time of the instrument was set to 200 μs, allowing the acquisition of spectra up to a mass/charge ratio of 1800 (data not shown). Mass-resolved images were taken at nominal mass resolution (burst alignment mode, focus 300 nm). A surface of $(90)^2$ μm^2 was rastered with 256×256 pixels (pixel size: 312 nm). The primary ion dose did not exceed 8×10^{12} ions/cm^2. In line with observations of Biesinger et al. (31), at this primary ion dose no change or inversion of contrast could be detected in any of the measurements performed.

Scanning force microscopy

Scanning force microscopy (SFM) images of the LB films transferred onto mica sheets were obtained at ambient conditions (20°C) using a Dimension 3100 scanning force microscope with a Nanoscope IIIa controller from Digital Instruments (Santa Barbara, CA) operating in tapping mode using PointProbe Plus(PPP) silicon tips (Nanosensors, Neuchatel, Switzerland) with a spring constant of 42 N/m. A detailed section height analysis was performed for all the images taken using WsXM/Nanoscope SFM software (freeware). Height scans from all the images were checked for analysis of variance and the obtained statistical histograms of section heights were analyzed using Gaussian functions to determine the average protrusion heights.

RESULTS

Chemical mapping of SP-B- and KL_4-containing surfactant model systems

Electrostatic interactions between cationic surfactant peptides such as SP-B and KL_4 and negatively charged DPPG are thought to exist in lipid/peptide monolayers and to affect lung surfactant function in vivo. Laterally resolved techniques such as ToF-SIMS, which allow for label-free detection of individual compounds of a monolayer, transferred to a solid support, should therefore enable us to uncover existent specific intermolecular interactions by means of chemical maps displaying distinct areas of colocalized species.

During ToF-SIMS analysis, a focused primary ion beam is rastered across the sample, leading to the release of compound characteristic secondary ions with different mass/charge (m/z) ratios and the pixel-by-pixel acquisition of mass spectra in

a defined area. Signal intensities for a given secondary ion are mapped in a way that brighter regions correspond to high ion counting rates. The obtained high-resolution mass images represent chemical maps semiquantitatively monitoring the distribution of the analyzed fragments. Since DPPC and DPPG, the two lipids used in our surfactant model systems, yield very similar mass fragments after surface bombardment (20,27), we typically use the palmitoyl chain-deuterated DPPG analog d62DPPG. Although the deuterated acyl chains of d62DPPG show a fragmentation pattern similar to the one of DPPC, the isotopic labeling results in significantly different secondary ion masses. The thus-obtained secondary ion signals therefore allow for unambiguous assignment of different lipid species to particular surface locations. Deuteration of DPPG does not alter its phase behavior or its miscibility with DPPC (as was previously demonstrated (27)).

The ToF-SIMS mass-resolved images obtained for DPPC/d62DPPG (4:1 molar ratio) LB-films containing 0.2 mol % SP-B (Fig. 1 *A*) or 0.4 mol % KL_4 (Fig. 1 *B*) reveal the lateral distribution of secondary ions (SI) typical for the different surfactant model compounds. Characteristic signals for DPPC result from cleavages in the lipid headgroup regions and yield fragments such as $C_5H_{12}NO^+$ with $m/z = 102$ u/e, also termed M102, or $C_5H_{14}NO^+$ with $m/z = 104$ u/e (M104) (Fig. 1 *A*). Further significant headgroup secondary ions are $C_2H_6PO_4^+$ (M125), $C_5H_{13}NPO_2^+$ (M150), or $C_8H_{19}NPO_4^+$ (M224), as well as the protonated and dehydrogenated quasimolecular ions $(DPPC\text{-}H)^+$ and $(DPPC{+}H)^+$ with nominal masses of 732.5 and 734.5 u/e, respectively (data not shown). All these secondary ions are found to be rather homogeneously distributed over the complete surface of samples containing SP-B, which is rather surprising since, in all our previously reported ToF-SIMS measurements, DPPC was localized in a network surrounding circular domains enriched in DPPG (or d62DPPG) together with the respective surfactant peptides (SP-B, SP-C, or KL_4) (20, 27–29). In the case of KL_4-containing films, the fact that DPPC forms bright domains surrounded by a darker network is even more unusual (Fig. 1 *B*), since it actually represents an inversion of lipid distribution compared to our previously reported studies performed in the presence of calcium ions (29). The addition of EDTA to the buffered subphase has a considerable effect on lipid/peptide mixing behavior, a point that is addressed in more detail in Discussion, below.

The interesting question now was whether we were able to finally detect colocalization of SP-B or KL_4 with anionic d62DPPG under conditions ensuring complete depletion of calcium ions in the subphase. d62DPPG, which does not yield any significant headgroup fragments (20), and is only identifiable by its deuterated acyl chain fragments such as $C_2D_5^+$ (M34) or $C_3D_7^+$ (M50) (Fig. 1). These fragments were found in distinct circular domains in monolayers containing SP-B (Fig. 1 *A*). The protein itself is identifiable by secondary ions originating from amino acids after cleavage of COOH. Typical fragments are $m/z = 30$ u/e (Gly), as displayed in Fig. 1 *A*, or M44 (Ala), M70 (Pro), M110 (His), and M120 (Phe), which also show a clear domain pattern in the ternary film (data not shown). Since the chemical maps obtained for d62DPPG and SP-B are rather diffuse, colocalization of these species cannot be revealed without further exploitation. We therefore performed a correlation analysis to unambiguously verify the lateral molecular distribution of all the surfactant compounds with respect to each other. The primary colors blue, green, and red were used to depict the chemical maps specific to DPPC, d62DPPG, and SP-B, respectively. A three-color overlay of the differently colored chemical maps then showed the respective lateral organization in terms of the fusion of the above primary colors. A superimposition of red and blue would give magenta-colored regions, red and green would result in yellow areas, and fusion of blue and green would appear as cyan. A colocalization of all three differently colored species would yield white areas. In the case of SP-B-containing lipid mixtures we indeed found yellow-colored regions indicative of a colocalization of SP-B and d62DPPG (Fig. 1 *A*). Additionally, magenta-colored regions surrounding yellow-colored domain areas were observed that could be attributed to the DPPC-rich lipid matrix, in which the d62DPPG/SP-B aggregates are embedded.

As mentioned above, in surfactant systems containing the model peptide KL_4 an unusual enrichment of DPPC in condensed regions surrounded by a dark networklike structure was found in the chemical maps of DPPC (Fig. 1 *B*). Verifying the lateral distribution of the d62DPPG-specific SI signals furnished further evidence for demixing of these two lipids and complete reversal of chemical distribution compared to LB-films transferred in the presence of calcium ions in the subphase (29). The KL_4 peptide, which only contains the amino acids leucine and lysine, is identified by the SI signals for these amino acids (e.g., M86 for Leu) and various species resulting from a more complex fragmentation pattern (e.g., M56, M70, M82, M84). The chemical map of, e.g., the KL_4-specific fragment M84 reveals that the peptide colocalizes with d62DPPG, a fact that is further confirmed by the correlation analysis presented in Fig. 1 *B*. This three-color overlay clearly shows the colocalization of KL_4 (*red*) with DPPG (*green*), giving rise to yellow-colored stretched domains.

Topography of lipid-protein model membranes containing SP-B and KL_4

During breathing, dynamic processes occur at the air/water interface that guarantee an efficient and controlled conversion of a surfactant monolayer completely covering the aqueous phase to a defined multilayered structure with the function of a surfactant reservoir (32). It has been shown previously that saturated lipids such as DPPC convey monolayer stability whereas unsaturated lipids are necessary for high flexibility of the surfactant film (4). Lipid/protein

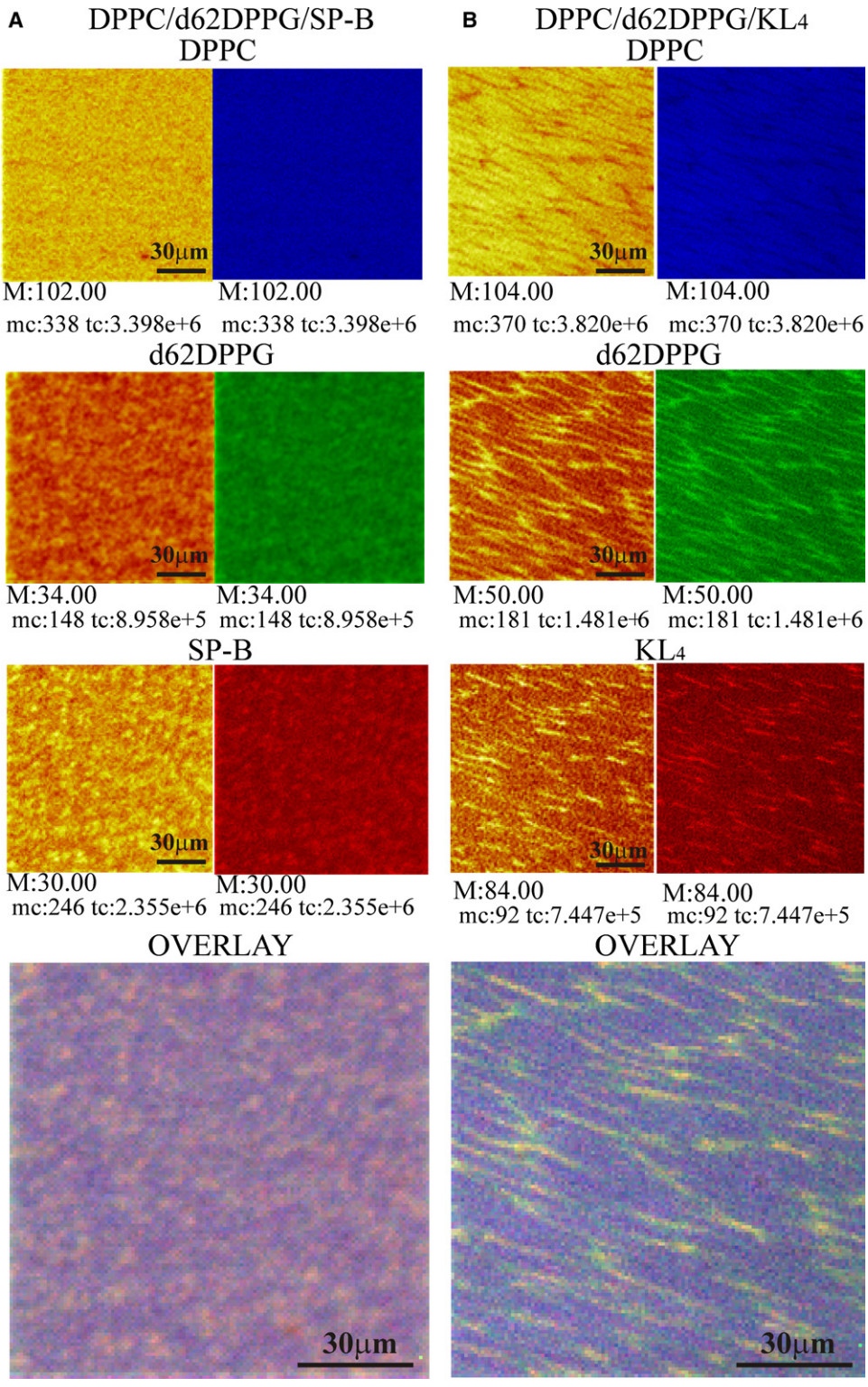

FIGURE 1 Mass-resolved ToF-SIMS images of surfactant monolayers consisting of (*A*) DPPC/d62DPPG/SP-B (4:1:0.2 mol %) and (*B*) DPPC/d62DPPG/KL_4 (4:1:0.4 mol %). LB-transfer was performed on to gold-covered glass slides at 50 mN/m from a subphase containing 25 mM HEPES, 0.1 mM EDTA (pH 7.0) at 20°C. The distributions of positively charged secondary ions deriving from DPPC ($m/z = 102, 104$), d62DPPG ($m/z = 34, 50$), SP-B ($m/z = 30$), and KL_4 ($m/z = 84$) are displayed in characteristic secondary ion intensity maps (*left rows*). The yellow/bright-colored regions suggest a higher intensity count of the secondary ion whereas brown/dark-colored regions denote a lower intensity count or absence of the same secondary ion. These images are also presented in different background primary colors (*right rows*) for correlation analysis represented by the large three-color overlay images obtained after overlapping the respective secondary ion maps with primary-color background.

interactions should have an influence on the molecular integrity as well as morphology of the protrusions formed under high surface pressure, a physical condition occurring, e.g., upon exhalation and decrease of lung surface area. Now that we were able to uncover conditions under which colocalization of SP-B or KL_4, with negatively charged lipid was discernible, we wanted to elucidate if depletion of subphase calcium not only resulted in changes in lipid/protein mixing behavior but also in surfactant layer morphology.

We therefore prepared solid supported LB-films by transfer of a surfactant monolayer at a film balance surface pressure of 50 mN/m and analyzed them by means of scanning

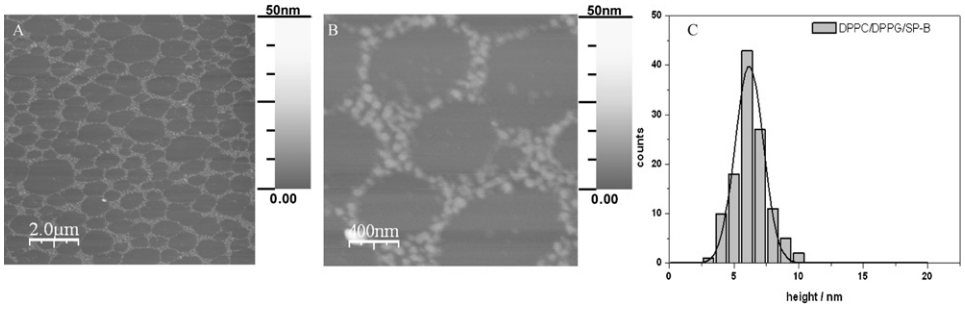

FIGURE 2 SFM topography images of monolayers consisting of DPPC/DPPG/SP-B (4:1:0.2 mol %). LB-films were transferred on to mica at a surface pressure of 50 mN/m from a subphase containing 25 mM HEPES, 0.1 mM EDTA (pH 7.0) at 20°C. All SFM images were taken in tapping mode (resolutions of (*A*) 10 × 10 μm^2 and (*B*) 2 × 2 μm^2). (*C*) Statistical histogram of protrusion heights by SFM section analysis. Average protrusion height was 6.1 ± 0.5 nm ($n = 115$).

force microscopy (SFM). The SFM images obtained for DPPC/DPPG monolayers containing 0.2 mol % SP-B are displayed in Fig. 2, *A* and *B*. Bright areas generally correspond to higher protrusions whereas dark regions represent structures of lower height. This is indicated by the grayscale bar next to the topographic images. In the case of SP-B-containing films, the formation of a polygonal network under calcium-free subphase conditions is visible. Such morphology is typical for SP-B and was found on pure water (33) as well as buffered subphases (28). Upon monolayer compression, lipids typically undergo a phase transition from a more fluid phase, termed liquid-expanded (LE) phase, to a tightly packed liquid-condensed (LC) phase (34). Peptides such as SP-B, SP-C, and even the smaller KL_4 are assumed to be excluded from these dense lipid domains and accumulate in the surrounding boundaries from which they are squeezed out at higher pressures together with lipid material (28,29,33). The former LC-phase is identified in SFM images as the flatter region of a defined diameter (SP-B-containing systems 3–10 μm on water (33) and 1–3 μm on buffer (28)). The squeezed-out material, however, is visible as three-dimensional structures forming a defined and more or less continuous network. These protrusions are found to be mostly of bilayer height (4–6 nm), indicating the importance of surfactant peptides for controlled and reversible material squeeze-out (28,33,35).

To further identify the influence of calcium depletion from the subphase on monolayer morphology and to quantify the three-dimensional structures observed in the SFM images, we performed a detailed statistical histogram analysis of protrusion heights. The statistical histogram obtained for SP-B-containing monolayers suggests a uniform distribution with an average protrusion height of 6.1 ± 0.5 nm (Fig. 2 *C*). This is typical of a bilayer thickness and is consistent with previously reported studies (28). The mean protrusion height was found to be statistically significant ($p < 0.05$). Although the average diameter of the LC domains was found to be 1–2 μm and comparable to previous studies (28), the lipid-protein clusters forming the disklike structure of the network were found to have a diameter of 110 ± 10 nm. Previous studies with SP-B carried out on water showed a cluster diameter of 55 ± 10 nm. This difference is probably due to the presence of a small amount of calcium ions in the water subphase (36) and is discussed later in further detail.

We next addressed the influence of calcium depletion on protrusion formation of KL_4-containing monolayers, which were transferred onto mica at a pressure of 50 mN/m. From our recent studies on KL_4 we know that the peptide induces the formation of flat and disorderedly arranged protrusions of stacked bilayers (7–12 nm height) and lipid-peptide aggregates (~3 nm height) in the presence of calcium (29). Our current results indicate that in KL_4-containing surfactant systems a continuous polygonal networklike structure is formed in the absence of divalent cations (Fig. 3, *A* and *B*). However, this network is not as pronounced as the one found in monolayers of native SP-B. The statistical analysis of section-heights suggest an average protrusion height of 9.5 ± 0.3 nm, which is statistically significant ($p < 0.05$) (Fig. 3 *C*). This height does not correspond to the typical thickness of a lipid bilayer membrane, an interesting feature that is addressed in further detail in the next section.

DISCUSSION

The lateral organization of lipids and proteins in a monolayer mainly depends on the physicochemical properties of the individual compounds, their mixing behavior, and the nature of interspecies interactions. Another important factor is the subphase onto which the lipid/protein film is spread, as well as its pH and the amount of mono- or divalent cations. The interfacial layer with all its possible electrostatic and hydrophobic interactions reigning between lipids and/or proteins as well as monolayer compounds and subphase ions is a highly complex system and difficult to judge on molecular levels. This complexity has to be kept in mind when discussing the existence of interactions between certain lipids and surfactant proteins and might be the reason why, despite the numerous studies of lipid mixtures with surfactant proteins, the existence of specific PG/SP-B interactions has so far, to our knowledge, never been unambiguously proven. Even now, in this study, we were only able to add further evidence for the existence of such specific interactions by revealing for the first time, to our knowledge, the unmistakable proof of colocalization of DPPG with SP-B or KL_4 under absolutely calcium-free conditions. It is important

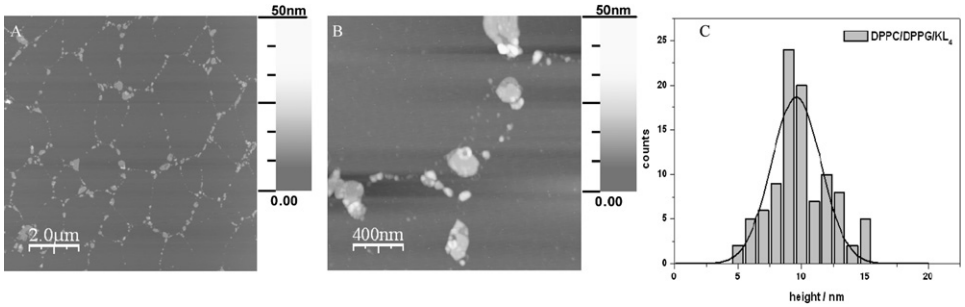

FIGURE 3 SFM topography images of monolayers consisting of DPPC/DPPG/KL_4 (4:1:0.4 mol %). LB-films were transferred on to mica at a surface pressure of 50 mN/m from a subphase containing 25 mM HEPES, 0.1 mM EDTA (pH 7.0) at 20°C. All the SFM images were taken in tapping mode (resolutions of (*A*) 10 × 10 μm^2 and (*B*) 2 × 2 μm^2). (*C*) Statistical histogram of protrusion heights by SFM section analysis. Average protrusion height was 9.5 ± 0.3 nm ($n = 93$).

to realize that depriving the calcium subphase conditions was aimed only to elucidate the possible influence of calcium ions—an idea that, again to our knowledge, has never been previously considered. In addition, in situ measured calcium contents are found to drastically vary during late gestation to infancy to adult (37)—making it highly complex, in a practical sense, to mimic the physiological ionic conditions. We will discuss our novel results considering our previous studies performed with ToF-SIMS as well as results of other research groups, hoping to shed some light on the mechanism of action leading the surfactant proteins to either colocalize with anionic DPPG or neutral DPPC.

Lipid-protein colocalization

In the studies performed so far trying to uncover the existence of specific DPPG/SP-B interactions, seemingly contradicting results were found. Analyzing surfactant model systems containing DPPC/DPPG (4:1 mol ratio) and 0.2 mol % SP-B on a pure water subphase (27) as well as on 0.1 mM HEPES with pH 5.5 or 7.0 (28) always delivered ToF-SIMS images bearing witness to a colocalization of positively charged SP-B with zwitterionic DPPC instead of negatively charged DPPG. Similar ToF-SIMS results were obtained for KL_4 on 25 mM HEPES at pH 7.0 this time, but in the presence of 3 mM $CaCl_2$ (29). These observations stand in clear contrast to the results from other groups supporting the idea of attractive electrostatic interactions prevailing between DPPG and SP-B. For example, Baatz et al. (38) concluded from fluorescence anisotropy studies with DPPC/DPPG (7:1) bilayers that SP-B selectively interacts with anionic lipids at pH 7 (120 mM NaCl, 10 mM MOPS) (13). Additionally, electron spin resonance spectroscopy studies on bilayer vesicular systems reported by Pérez-Gil et al. indicated the existence of SP-B/DPPG interaction at pH 7 (50 mM HEPES, 150 mM NaCl, 5 mM EDTA) (25). Interestingly, no preferential interaction of SP-B with either DPPC or DPPG was observed in bilayers studied by means of ^2H NMR at pH ~7 (15 mM HEPES, 135 mM NaCl) (26), even though these measurements also used vesicular systems and solutions with high ionic strength.

A possible explanation for the observed difference could be that different model membranes were used, e.g., monolayer systems spread on an aqueous subphase in our previous studies and bilayer structures in the mentioned investigations. One could argue that SP-B adopts different conformations in monolayer and in bilayer environments due to differences in membrane thickness. Such observations have been reported previously for SP-B peptides (39). However, if we consider the fact that lipids in monolayers compressed to surface pressures well above 30 mN/m are in a similar condensed state to lipids in vesicle bilayers (40,41), and that the amphiphilic SP-B is mainly located in the phospholipid headgroup region (13,42), the reason for the difficulties identifying colocalization of SP-B with DPPG must lie elsewhere. The most obvious explanation would be that electrostatic interactions at the air/water interface play a crucial role in the lateral organization of the monolayer. This conclusion is based on several observations made in our previous studies. We reported that a hydrogen-bonding network probably exists that bridges negatively charged lipids, and thus reduces the solubility of SP-B in such densely packed regions (28). This network obviously includes the glycerol-containing lipid headgroups, as was evidenced by infrared spectroscopy (43,44). Such a hydrogen-bonding network will promote the formation of tight DPPG-rich domains from which other lipid and protein species will be excluded. It is conceivable that under such conditions no colocalization of SP-B with a negatively charged lipid would exist. The extension of such a network and its potency to induce the formation of condensed DPPG domains will naturally depend on the pH as well as the ionic strength of the solution. Since the studies from Baatz et al. (13) and Pérez-Gil et al. (25) were performed at a different pH than our measurements and their solutions contained NaCl unlike ours, it is possible that in their case the hydrogen-bonding network was disrupted due to electrostatic interactions between subphase ions and lipid headgroups. Monovalent cations tend to stabilize the so-called liquid-expanded phase of lipid monolayer by penetrating into the headgroup region of DPPG (45). It is very likely that in the presence of NaCl, DPPG exists in more fluid phase enabling SP-B or KL_4 to interact with the negatively charged headgroups by predominant electrostatic interaction.

Furthermore, we demonstrated in ToF-SIMS measurements with LB-films containing DPPC and anionic dipalmitoylphosphatidylserine, which were transferred on gold substrates from a pure water subphase, that calcium ions

were always detectable in PS-rich regions unless ethylene glycol tetraacetic acid was added to the solution (36). These results made it plain that the slightest traces of calcium ions remain in the aqueous phase if no chelating agent is present and that these divalent cations inevitably bind to negatively charged lipids present in the monolayer. Such a scenario is also conceivable for DPPG-containing monolayers (22), which would entail the calcium-induced formation of DPPG-rich domains from which DPPC and SP-B are excluded, as was recently demonstrated in our study of KL_4 in the presence of calcium ions (29). Consequently, when trying to explain the lateral distribution of lipids and proteins, not only the influence of a hydrogen-bonding network but also the effect of even the smallest traces of calcium ions, have to be considered.

To definitely exclude the influence of calcium ions on the mixing behavior of our surfactant model system we decided to choose the experimental conditions of our previous KL_4 study (25 mM HEPES, pH 7.0) and to add EDTA instead of 3 mM $CaCl_2$. And indeed, in the SP-B containing system, we were still able to demonstrate the disappearance of the typical DPPG-rich domains we have always been able to detect. Instead, a more homogeneously distributed and better-mixed monolayer seems to exist. The addition of EDTA to the buffered subphase leads to a fluidization of the surfactant monolayer, most likely due to the chelation of calcium ions but also because of its negatively charged carboxylate groups having a repulsive effect on the anionic phosphate lipid headgroups. Under such conditions, specific interactions between SP-B and DPPG are most likely to exist. This is in line with the previous studies showing localization of SP-B and other protein with the disordered phase comprised largely of the unsaturated lipid suggesting the significance of fluidity (46,47). In the case of the model peptide KL_4, we were finally able to detect a clear colocalization with DPPG. The increased charge/mass ratio of KL_4 compared to SP-B probably leads to stronger electrostatic interactions with negatively charged DPPG, and thus to a more pronounced formation of lipid/peptide complexes which are laterally separated from DPPC-rich domains. The observed stretched domains forming the polygonal network are difficult to explain, but could be attributed to the fusion of adjacent boundaries; however, further research on the occurrence of stretched domains is needed to explain such shapes clearly.

Protrusion formation in a calcium-free system

Most of the existing lipid-protein interactions drive important functions. In this context, both SP-B and the mimic peptide KL_4 are essential for the formation of the so-called surface-associated surfactant reservoir at the alveolar interface (29,33,35,48). SP-B is found to induce formation of bilayer membrane protrusions of ~6 nm height and a diameter of 55 $\pm$ 10 nm (33). These three-dimensional structures are formed upon compression of the monolayer when LC ''islands'' containing tightly packed lipids collide and the larger proteins enriched in the surrounding fluid matrix start to dive into the subphase (a process also termed ''squeeze-out'', at higher surface pressures) (33,48). The absence of divalent cations thus seems to have no effect on the peptides' functional activity. Both SP-B and KL_4 promote the formation of protrusions arranged in an interconnected networklike structure. In the case of SP-B, protrusion height was 6.1 $\pm$ 0.5 nm, a value typical for this protein. Only the protrusion diameter was found to be distinctly larger, at 110 $\pm$ 10 nm (28,33). This increase in protrusion size could be due to the absence of divalent cations leading to the stabilization of the LE-state of DPPG, as there is no bridging of the negatively charged headgroups.

Interestingly, in the absence of divalent cations the peptide KL_4 is able to form an interconnected networklike structure similar to SP-B and not the disorderedly structured domains that we observed in the presence of divalent cations. We assume that adding EDTA to the subphase leads to a more homogeneously distributed peptide in the monolayer, and additionally inhibits the observed calcium induced aggregation of KL_4. Most importantly, however, removing calcium ions from the subphase leads to significant differences in protrusion morphology. For example, the observed protrusion height of 9.5 $\pm$ 0.3 nm does not correspond to the typical value of 5–6 nm for a lipid bilayer. However, the overall appearance of the protrusions formed in KL_4/lipid layers does resemble the bilayer structures observed in SP-C-containing systems (48) as well as in DPPG/KL_4 mixtures in the presence of calcium (29). The dimensions of the found patches in calcium free KL_4-systems (diameters up to 200 nm) as well as their flatness indicates that these too are composed of lipid bilayers. Since we postulated that negatively charged lipids are necessary for the formation of bilayer structures (29) and DPPG is colocalized with KL_4 under calcium free conditions, we therefore assume that, indeed, bilayers are formed and that the increased height of the observed three-dimensional structures is probably due to an intercalation of anionic EDTA between adjacent lipid layers increasing the repulsive forces already existing between neighboring DPPG molecules. It is also possible that KL_4 stabilizes lipid bilayer patches not in a way that is postulated for native SP-B by an attachment to protrusion rims (33) but instead by partially intercalating into adjacent lipid layers and bridging neighboring DPPG headgroups. Such a behavior would also lead to an increased height of bilayer protrusions. In addition, it has to be considered that KL_4 is characterized by high conformational flexibility, which can be switched from α-helix to β-sheet by the addition of calcium ions or by other factors such as increasing surface pressure or lipid packing density (49,50). It is not clear, however, how such a conformational change would influence the morphology or the height of the protrusions formed in the presence of KL_4. It has even been reported

that KL_4 adopts a transmembrane orientation despite the presence of charged lysine residues in microsomal membrane preparations (51). Such a behavior, so far, has not been considered in our explanation of height differences, and has to be elucidated by further studies on KL_4 conformation in surfactant monolayers under calcium free conditions. Another surprising hint that arises from the reversal of the protein colocalization with the lipids as a consequence of different ionic environment is in direct confrontation with the unanimity of the ''squeeze-out theory'', according to which only the non-DPPC lipids are selectively squeezed out from the surface into the surfactant reservoir facilitated by the protein. Although the squeeze-out theory has been generally applied to interpret the observations in the lung surfactant experiments, there is, however, no convincing evidence on the squeeze-out phenomenon and the fate of squeezed-out lipids and protein (52,53). Our results show that specificity of interactions, and thus, possibly selectivity of the lipids being squeezed out, could depend on the fluidity of the lipid domains. It is, therefore possible that, under varying ionic conditions, both DPPC and DPPG could be squeezed out along with the protein. This is in line with other studies that proposed a protein-induced alteration of phase behavior of the lipids, eliminating the need for selective squeeze-out (8,14,54,55). Additionally, it would be interesting to test our hypothesis by investigating a mixture of saturated and unsaturated lipids to see whether the subsequent fluidity drives protein localization.

CONCLUSION

Together, we show here that colocalization of SP-B or KL_4 with certain phospholipids depends on lipid fluidity and the miscibility of all surfactant components, which in turn depends on the ionic environment. The reversal of the protein colocalization with either DPPC or DPPG and the peptide's membrane protrusion-forming ability thus depend on the presence of calcium ions, which seem to act as a ''miscibility switch'' and to be one of the major factors steering the mixing behavior of DPPG in a DPPC/protein matrix. Understanding the driving forces behind phase behavior and mixing processes will always be of importance not only for surfactant model systems but for any lipid protein mixture, and will remain one of the main challenges for research.

We thank Prof. Richard Mendelsohn from the Department of Chemistry, Rutgers University, for providing us with the peptide KL_4, and Tascon GmbH, Münster, Germany.

This work was supported by the NRW Graduate School of Chemistry (to M.S.) and the Deutsche Forschungsgemeinschaft as a contribution from Sonderforschungsbereich (grant No. 424/B9 to H.-J.G.).

REFERENCES

1. Goerke, J. 1974. Lung surfactant. *Biochim. Biophys. Acta*. 344:241–261.
2. Yu, S., P. G. Harding, N. Smith, and F. Possmayer. 1983. Bovine pulmonary surfactant: chemical composition and physical properties. *Lipids*. 18:522–529.
3. Holm, B. A., Z. Wang, E. A. Egan, and R. H. Notter. 1996. Content of dipalmitoyl phosphatidylcholine in lung surfactant: ramifications for surface activity. *Pediatr. Res.* 39:805–811.
4. Veldhuizen, R., K. Nag, S. Orgeig, and F. Possmayer. 1998. The role of lipids in pulmonary surfactant. *Biochim. Biophys. Acta*. 1408:90–108.
5. Cockshutt, A. M., D. R. Absolom, and F. Possmayer. 1991. The role of politic acid in pulmonary surfactant: enhancement of surface activity and prevention of inhibition by blood proteins. *Biochim. Biophys. Acta*. 1085:248–256.
6. Creuwels, L. A., L. M. van Golde, and H. P. Haagsman. 1997. The pulmonary surfactant system: biochemical and clinical aspects. *Lung*. 175:1–39.
7. Yu, S. H., and F. Possmayer. 2003. Lipid compositional analysis of pulmonary surfactant monolayers and monolayer-associated reservoirs. *J. Lipid Res*. 44:621–629.
8. Ding, J., D. Y. Takamoto, A. von Nahmen, M. M. Lipp, K. Y. Lee, et al. 2001. Effects of lung surfactant proteins, SP-B and SP-C, and palmitic acid on monolayer stability. *Biophys. J*. 80:2262–2272.
9. Hawgood, S., M. Derrick, and F. Poulain. 1998. Structure and properties of surfactant protein B. *Biochim. Biophys. Acta*. 1408:150–160.
10. Kuroki, Y., and D. R. Voelker. 1994. Pulmonary surfactant proteins. *J. Biol. Chem*. 269:25943–25946.
11. Nag, K., S. G. Taneva, J. Pérez-Gil, A. Cruz, and K. M. Keough. 1997. Combinations of fluorescently labeled pulmonary surfactant proteins SP-B and SP-C in phospholipid films. *Biophys. J*. 72:2638–2650.
12. Oosterlaken-Dijksterhuis, M. A., M. van Eijk, L. M. van Golde, and H. P. Haagsman. 1992. Lipid mixing is mediated by the hydrophobic surfactant protein SP-B but not by SP-C. *Biochim. Biophys. Acta*. 1110:45–50.
13. Baatz, J. E., B. Elledge, and J. A. Whitsett. 1990. Surfactant protein SP-B induces ordering at the surface of model membrane bilayers. *Biochemistry*. 29:6714–6720.
14. von Nahmen, A., A. Post, H. J. Galla, and M. Sieber. 1997. The phase behavior of lipid monolayers containing pulmonary surfactant protein C studied by fluorescence light microscopy. *Eur. Biophys. J*. 26:359–369.
15. Wang, Z., S. B. Hall, and R. H. Notter. 1995. Dynamic surface activity of films of lung surfactant phospholipids, hydrophobic proteins, and neutral lipids. *J. Lipid Res*. 36:1283–1293.
16. Cochrane, C. G., and S. D. Revak. 1991. Pulmonary surfactant protein B (SP-B): structure-function relationships. *Science*. 254:566–568.
17. Ma, J., S. Koppenol, H. Yu, and G. Zografi. 1998. Effects of a cationic and hydrophobic peptide, KL4, on model lung surfactant lipid monolayers. *Biophys. J*. 74:1899–1907.
18. Sarin, V. K., S. Gupta, T. K. Leung, V. E. Taylor, B. L. Ohning, et al. 1990. Biophysical and biological activity of a synthetic 8.7-kDa hydrophobic pulmonary surfactant protein SP-B. *Proc. Natl. Acad. Sci. USA*. 87:2633–2637.
19. Bruni, R., H. W. Taeusch, and A. J. Waring. 1991. Surfactant protein B: lipid interactions of synthetic peptides representing the amino-terminal amphipathic domain. *Proc. Natl. Acad. Sci. USA*. 88:7451–7455.
20. Bourdos, N., F. Kollmer, A. Benninghoven, M. Ross, M. Sieber, et al. 2000. Analysis of lung surfactant model systems with time-of-flight secondary ion mass spectrometry. *Biophys. J*. 79:357–369.
21. Oosterlaken-Dijksterhuis, M. A., H. P. Haagsman, L. M. van Golde, and R. A. Demel. 1991. Characterization of lipid insertion into monomolecular layers mediated by lung surfactant proteins SP-B and SP-C. *Biochemistry*. 30:10965–10971.
22. Oosterlaken-Dijksterhuis, M. A., H. P. Haagsman, L. M. van Golde, and R. A. Demel. 1991. Interaction of lipid vesicles with monomolecular layers containing lung surfactant proteins SP-B or SP-C. *Biochemistry*. 30:8276–8281.

23. Yu, S. H., and F. Possmayer. 1990. Role of bovine pulmonary surfactant-associated proteins in the surface-active property of phospholipid mixtures. *Biochim. Biophys. Acta.* 1046:233–241.
24. Curstedt, T., and J. Johansson. 2006. New synthetic surfactant—how and when? *Biol. Neonate.* 89:336–339.
25. Pérez-Gil, J., C. Casals, and D. Marsh. 1995. Interactions of hydrophobic lung surfactant proteins SP-B and SP-C with dipalmitoylphosphatidylcholine and dipalmitoylphosphatidylglycerol bilayers studied by electron spin resonance spectroscopy. *Biochemistry.* 34:3964–3971.
26. Dico, A. S., J. Hancock, M. R. Morrow, J. Stewart, S. Harris, et al. 1997. Pulmonary surfactant protein SP-B interacts similarly with dipalmitoylphosphatidylglycerol and dipalmitoylphosphatidylcholine in phosphatidylcholine/phosphatidylglycerol mixtures. *Biochemistry.* 36:4172–4177.
27. Breitenstein, D., J. J. Batenburg, B. Hagenhoff, and H. J. Galla. 2006. Lipid specificity of surfactant protein B studied by time-of-flight secondary ion mass spectrometry. *Biophys. J.* 91:1347–1356.
28. Seifert, M., D. Breitenstein, U. Klenz, M. C. Meyer, and H. J. Galla. 2007. Solubility versus electrostatics: what determines lipid/protein interaction in lung surfactant. *Biophys. J.* 93:1192–1203.
29. Saleem, M., M. C. Meyer, D. Breitenstein, and H. J. Galla. 2008. The surfactant peptide KL4 in lipid monolayers: phase behavior, topography, and chemical distribution. *J. Biol. Chem.* 283:5195–5207.
30. Haagsman, H. P., S. Hawgood, T. Sargeant, D. Buckley, R. T. White, et al. 1987. The major lung surfactant protein, SP 28–36, is a calcium-dependent, carbohydrate-binding protein. *J. Biol. Chem.* 262:13877–13880.
31. Biesinger, M. C., P. Y. Paepegaey, N. S. McIntyre, R. R. Harbottle, and N. O. Petersen. 2002. Principal component analysis of TOF-SIMS images of organic monolayers. *Anal. Chem.* 74:5711–5716.
32. Schurch, S., R. Qanbar, H. Bachofen, and F. Possmayer. 1995. The surface-associated surfactant reservoir in the alveolar lining. *Biol. Neonate.* 67 (Suppl 1):61–76.
33. Krol, S., M. Ross, M. Sieber, S. Kunneke, H. J. Galla, et al. 2000. Formation of three-dimensional protein-lipid aggregates in monolayer films induced by surfactant protein B. *Biophys. J.* 79:904–918.
34. Mohwald, H. 1990. Phospholipid and phospholipid-protein monolayers at the air/water interface. *Annu. Rev. Phys. Chem.* 41:441–476.
35. Diemel, R. V., M. M. Snel, A. J. Waring, F. J. Walther, L. M. van Golde, et al. 2002. Multilayer formation upon compression of surfactant monolayers depends on protein concentration as well as lipid composition. An atomic force microscopy study. *J. Biol. Chem.* 277:21179–21188.
36. Ross, M., C. Steinem, H.-J. Galla, and A. Janshoff. 2001. Visualization of chemical and physical properties of calcium-induced domains in DPPC/DPPS Langmuir-Blodgett layers. *Langmuir.* 17:2437–2445.
37. Eckenhoff, R. G. 1989. Perinatal changes in lung surfactant calcium measured in situ. *J. Clin. Invest.* 84:1295–1301.
38. Baatz, J. E., V. Sarin, D. R. Absolom, C. Baxter, and J. A. Whitsett. 1991. Effects of surfactant-associated protein SP-B synthetic analogs on the structure and surface activity of model membrane bilayers. *Chem. Phys. Lipids.* 60:163–178.
39. Dieudonne, D., R. Mendelsohn, R. S. Farid, and C. R. Flach. 2001. Secondary structure in lung surfactant SP-B peptides: IR and CD studies of bulk and monolayer phases. *Biochim. Biophys. Acta.* 1511:99–112.
40. Hui, S. W., M. Cowden, D. Papahadjopoulos, and D. F. Parsons. 1975. Electron diffraction study of hydrated phospholipid single bilayers. Effects of temperature hydration and surface pressure of the "precursor" monolayer. *Biochim. Biophys. Acta.* 382:265–275.
41. Owicki, J. C., M. W. Springgate, and H. M. McConnell. 1978. Theoretical study of protein-lipid interactions in bilayer membranes. *Proc. Natl. Acad. Sci. USA.* 75:1616–1619.
42. Morrow, M. R., J. Perez-Gil, G. Simatos, C. Boland, J. Stewart, et al. 1993. Pulmonary surfactant-associated protein SP-B has little effect on acyl chains in dipalmitoylphosphatidylcholine dispersions. *Biochemistry.* 32:4397–4402.
43. Dicko, A., T. Di Paolo, and M. Pezolet. 1998. Interaction of dehydroepiandrosterone with phospholipid membranes: an infrared spectroscopy investigation. *Biochim. Biophys. Acta.* 1368:321–328.
44. Blume, A., W. Hubner, and G. Messner. 1988. Fourier transform infrared spectroscopy of 13C = O-labeled phospholipids hydrogen bonding to carbonyl groups. *Biochemistry.* 27:8239–8249.
45. Maltseva, E., V. L. Shapovalov, H. Mohwald, and G. Brezesinski. 2006. Ionization state and structure of l-1,2-dipalmitoylphosphatidylglycerol monolayers at the liquid/air interface. *J. Phys. Chem. B.* 110:919–926.
46. Takamoto, D. Y., M. M. Lipp, A. von Nahmen, K. Y. Lee, A. J. Waring, et al. 2001. Interaction of lung surfactant proteins with anionic phospholipids. *Biophys. J.* 81:153–169.
47. Ding, J., I. Doudevski, H. E. Warriner, T. Alig, J. A. Zasadzinski, et al. 2003. Nanostructure changes in lung surfactant monolayers induced by interactions between palmitoyloleoylphosphatidylglycerol and surfactant protein B. *Langmuir.* 19:1539–1550.
48. Amrein, M., A. von Nahmen, and M. Sieber. 1997. A scanning force- and fluorescence light microscopy study of the structure and function of a model pulmonary surfactant. *Eur. Biophys. J.* 26:349–357.
49. Cai, P., C. R. Flach, and R. Mendelsohn. 2003. An infrared reflection-absorption spectroscopy study of the secondary structure in (KL4)4K, a therapeutic agent for respiratory distress syndrome, in aqueous monolayers with phospholipids. *Biochemistry.* 42:9446–9452.
50. Saenz, A., O. Canadas, L. A. Bagatolli, M. E. Johnson, and C. Casals. 2006. Physical properties and surface activity of surfactant-like membranes containing the cationic and hydrophobic peptide KL4. *FEBS J.* 273:2515–2527.
51. Martinez-Gil, L., J. Pérez-Gil, and I. Mingarro. 2008. The surfactant peptide KL4 sequence is inserted with a transmembrane orientation into the endoplasmic reticulum membrane. *Biophys. J.* 95:L36–L38.
52. Bangham, A. D., C. J. Morley, and M. C. Phillips. 1979. The physical properties of an effective lung surfactant. *Biochim. Biophys. Acta.* 573:552–556.
53. Goerke, J. 1998. Pulmonary surfactant: functions and molecular composition. *Biochim. Biophys. Acta.* 1408:79–89.
54. Lipp, M. M., K. Y. C. Lee, D. Y. Takamoto, J. A. Zasadzinski, and A. J. Waring. 1998. Coexistence of buckled and flat monolayers. *Phys. Rev. Lett.* 81:1650–1653.
55. Crane, J. M., and S. B. Hall. 2001. Rapid compression transforms interfacial monolayers of pulmonary surfactant. *Biophys. J.* 80:1863–1872.